# Risk Level Analysis for Hazard Area During Commercial Space Launch

Oliver J. Bojorquez
*Department of Aerospace Engineering*
*San Diego State University*
San Diego, CA, 92182-1308
obojorquez@sdsu.edu

Jun Chen
*Department of Aerospace Engineering*
*San Diego State University*
San Diego, CA, 92182-1308
jun.chen@sdsu.edu

***Abstract*—Current method used for integrating space launch vehicles into National Airspace System (NAS) and reducing aircraft risks includes closing large air space areas to any air vehicles, known as hazard areas. Airspace regulations cause aircraft to reroute increasing flight distance, delays and overall flight cost. Air space restriction area and time are based on profile risk factors of space vehicle launch. This paper describes a method to dynamically construct a risk level map of commercial space launch operations' impact on nearby aircraft. The hazard area is divided into multiple sections, each section is also dynamically evaluated for a risk level, which is a comprehensive index considering the uncertain debris trajectory model and launch failure probabilities. This method provides a framework for modeling an optimal aircraft routing plan within a required risk level.**

***Index Terms*—Space launch, Risk analysis, Monte Carlo simulation, Hazard area**

## I. Introduction

To safely integrate space launch operations into air traffic flow and minimize the risk to aircraft from potential accidents, Federal Aviation Administration (FAA) creates blocks of space surrounding the trajectory of the space vehicle for an extended amount of time. These blocks serve as a temporary flight restriction area covering a vast range, from launch pad to an altitude of 30 nautical miles, prohibiting all air vehicles from crossing this restricted area. Aviation restriction is generally activated 7 hours prior to launch and stays in effect 30 minutes after launch [1]–[3]. These restricted areas force air traffic flow to reroute around hazard areas, resulting in delays, increased fuel consumption and over all operational cost per flight. Delayed flights not only increase the aircrafts operational cost (maintenance, fuel, crew, etc.) it also requires ground personnel, extra gates and other external needs necessary to maintain a reasonable traffic flow [1].

With increasing demands in space access for commercial and military purposes these restricted areas will inevitably become more frequent and cause a substantial impact on air traffic flow [4]. Typically flight delays caused by these restricted zones would have overall operational cost increase averaging out in thousands per flight [5]. According to Airlines for America in 2018 average estimated cost of aircraft delay was 74.20 dollars per minute plus additional cost due to external costs [6]: decrease in airline demand, ground labor, etc. The overall cost could reach billions annually. Therefore, an increase in space exploration also demands appropriate methods to maintain an efficient traffic flow.

Beyond there is an increase demand in space launch operations, inevitably a steady increase in number of aircraft in airspace will also occur. Increase of number of aircraft in the airspace causes a linear overall cost increase. Air Route Traffic Control Centers (ARTCC) provides forecasts of projected increase of aircraft in the air space. These forecasts serve as a base to determine future requirements regarding facilities, equipment, manpower and other related services [7]. According to FAA aerospace Forecasts Fiscal Years 2019-2039 [4] projected increase in aircraft annually is 1.4 percent. This steady increase implies a larger number of aircraft impacted by hazard areas making traffic flow much more difficult to evaluate.

To allocate the various air space and other sources to maintain an efficient traffic flow, Traffic Flow Management (TFM) is an efficient tool used by FAA. This task is accomplished by using a system approach managed by traffic personnel to facilitate the flow. These personnel analyze knowledge sent to them by en route and terminal controllers as well as other programs such as miles in trail (MIT), ground delay programs (GDP), ground stop (GS) and others to coordinate efficiently in the decision-making process [8]. In addition to regulating traffic flow involving arriving and departing flights, traffic management over constrained regions in NAS requires rerouting around blocked regions. These regions are air space regions blocked due to severe weather or other events which historically have caused an influence on air traffic flow. Routes used around these spaces are validated by ARTCC, these collections of routes known as National Playbook intended to assist traffic flow personnel conducting decisions, for this paper the most relevant routes are those involving operations inside blocked areas.

Although, TFM remains a complex area of study presented with several challenges ranging from human factors to software engineering, continuous research in this discipline has aided in obtaining more efficient traffic flow. However, the current method with deterministic forbidden area provides little flexibility for TFM on hazard area. As launch operation demands increase, the need for a more flexible and risk level

guaranteed TFM tool to increase the operational efficiency of the hazard area will become apparent.

Since the newborn space transport industry is still in its very early stage, there is limited previous studies that have focused on the integration of space traffic into NAS. Previous works at Stanford [5], [9]–[11] provide some preliminary guidance for this emerging area. In specific, the work in [9] formulated the optimal aircraft routing problem during space launches as a Markov Decision Process (MDP) to model the stochastic nature of possible debris. Later, an efficient method based on adaptive spatial discretization is proposed to handle the computational tractability [10]. To help easily evaluate the impact of a launch anomaly, some useful tools for safety range are introduced in [5], [11]. However, all the above works handle the problem as a static collision avoidance problem. To the best of the author's knowledge, there exists little research considering dynamical risk tolerance for aircraft rerouting during the space launches. This paper aim to bridge this research gap.

To achieve the risk level guaranteed aircraft rerouting plan, this paper presents a proficient and accurate method to obtain a dynamically updated risk level map of hazard area during space launch. Then a simple risk based rerouting plan is proposed for illustration. To further increase credibility and accuracy of data, launch used on this paper is a hypothetical scenario which involves vehicle launched from Cape Canaveral Spaceport following a representative two stage to orbit trajectory and its impacts on air traffic at 31,000 feet. Scenario allows genuine debris uncertainty model projected over a risk level map. The risk level is a comprehensive index, which considers debris model with uncertainty and historical launch failure probabilities. More importantly, the risk level map can be easily transformed as a joint probability distribution of risk, which is a key component for risk-bounded stochastic planning [8] for aircraft rerouting.

## II. Problem Formulation for Risk Assessment

To better evaluate the risk to aircraft, the hazard area is divided into multiple sections by building a grid mesh, each section is dynamically evaluated for a risk level (as shown in Fig. 1) by a Monte Carlo based simulation. The risk level is a comprehensive index, which has two parts: Debris model and Launch failure probabilities. Each section requires several factors which directly depicts the risk level awarded to each section when building the grid mesh.

### A. Debris model

Debris model is a major component to calculate the chance each section will be hit. Creating a grid displaying probable area hit, allows accurate risk level consideration involving debris trajectory. Model used to provide results of debris impacted area is a commercial spacecraft launched form Cape Canaveral following a two-stage trajectory. This spaceport is the primary launch site for the united states, having a high number of Space launches every year taking advantage of its proximity to the ocean and benefiting from the earths rotation makes this location ideal to conduct hypothetical scenarios.

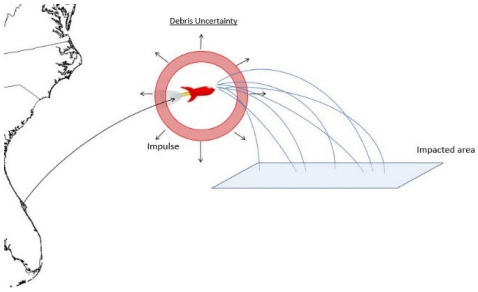


Fig. 1: Debris uncertainty representation of impacted area of air space.

Although previous studies have presented debris trajectory, weather conditions and nearby impacted area [11], approach provided in this paper can efficiently evaluate the debris footprint on commercial flight level using a Monte Carlo simulation. Impacted profile is assessed using following parameters: randomly given mass, number of debris pieces, velocity, wind direction and speed, air density at different altitudes and explosion impulses.

Forces addressed to develop these equations of motion are lift, drag, and weight of each piece. Simulation is intended to represent a space launch operation dispersing onto a randomize number of pieces, still abiding by the laws of physics. Mass can not be created or destroyed therefore system will follow thes conservation of mass principle:

$$m_{total} = \sum_{i \in N} m_i \tag{1}$$

where total mass ($m_{total}$) is recognized as the weight vehicle had at moment of of incident. Accident would contain a random number of debris selection where total mass need to remain roughly unchanged for any number of debris. Similarly, to maintain the same total momentum of the system, the law of momentum conservation is obeyed as well:

$$m_{total} V_0 = \sum_{i \in N} m_i V_i \tag{2}$$

where $V_i$ is calculate based on the initial velocity ($V_0$) and the impulse speed from explosion.

#### *Debris Propagation Trajectory Dynamics*

The debris piece travelling over a spherical rotating Earth follows a point mass dynamics. The set of 3 degree of freedom (3DOF) equations of motion is described as following:

$$\dot{r} = V \sin\gamma \tag{3}$$

$$\dot{\theta} = \frac{V \cos\gamma \sin\psi}{r \cos\phi} \tag{4}$$

$$\dot{\phi} = \frac{V \cos\gamma \cos\psi}{r} \tag{5}$$

$$\dot{V} = \frac{L - D}{m} - g \sin\gamma + r\Omega^2 \cos\phi(\sin\gamma \cos\phi - \sin\phi \sin\psi \cos\gamma) \tag{6}$$

Where $r$ is the radial distance from the Earth centre to the vehicle, $V$ is the Earth-relative velocity, $\theta$ and $\phi$ are the geodetic longitude and latitude, respectively, $\gamma$ is the flight-path angle, and $\psi$ is the velocity heading (track) angle. $g$ is the gravitational acceleration, and $\Omega$ is the Earth's self-rotation rate, m is the vehicle mass.

L and D are the lift and drag, respectively:

$$L = \frac{1}{2}\rho V_R^2 S C_L(V) \tag{7}$$

$$D = \frac{1}{2}\rho V_R^2 S C_D(V) \tag{8}$$

Here $\rho$ is the air density which is varying along altitude, $S$ is the reference area, $C_L$, $C_D$ are the lift and drag coefficients respectively and $V_R$ is the velocity relative to the wind: $V_R = V - V_{wind}$. We assume the aerodynamics coefficients depend only on velocity (Mach number).

Note that velocity is on a continuous change throughout trajectory with each debris affected by a change in wind speed ($V_{wind}$). Following the dynamics functions, simulation must display behavior similar to the image shown in figure 1.

*Debris Hit Map*

The above debris propagation model will describe the behavior of each debris. For demonstration, model in this paper is set to mimic the space launch operation of a vehicle with maximum initial mass of 30,000 kilograms. To simplify the process, a rocket simulation is modeled accounting for gravitational, drag and thrust forces to appropriately render the motion. simulation is stopped at different times, retrieving location, mass and velocity of rocket. These points are used to represent different accident scenarios where debris uncertainty projectile is established to have random debris breakdown dispersing into any size, shape, mass, speed and direction. Including additional speed added by explosion, projectile would be heavily impacted by a randomized change in wind direction rendering range of debris uncertainty.

Trajectory for any unprecedented debris is calculated with its final point of interested set at normal cruise altitude for commercial aircraft (31,000 ft). Using this uncertainty method an algorithm was developed to process this debris trajectory multiple times. Running this algorithm for an extended number in parallel increases the accuracy of probable area hit by debris.

Having a debris hit map displaying the numerous locations these randomize pieces land allows us to develop a heat map demonstrating which area is most probable to be hit. Setting these locations on a coordinate system following intended trajectory over the Atlantic Ocean, images shown in figure 2 represent algorithm processed five hundred times illustrating a scatter plot of all probable locations of debris.

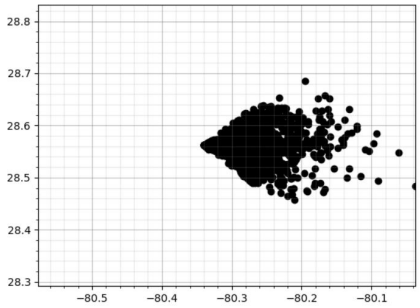


(a) Scatter map

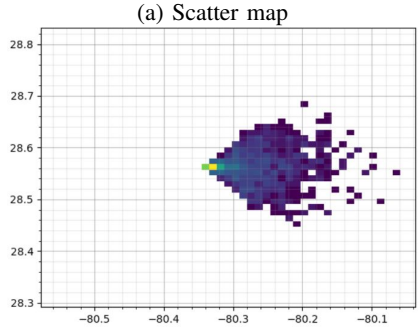


(b) Heat Map

Fig. 2: Scatter and heat map of debris impacted area.

In figure 2, all values retrieved are graphed on a longitude and latitude coordinate system. Dividing these heat maps into blocks of space with each block containing probable value of debris hitting this range, in this paper grid map is divided as a 50x50 evenly size blocks of space. Creating this grid is critical when evaluating a risk level, each block of space contains risk level assign to them which would contain an additional factor, historical launch failure probabilities. These blocks serve as hazard areas for the rerouting.

*B. Launch failure probabilities*

Launch failure probabilities are categorized in different phases of trajectory using historical data identifying time and position failures are more probable to occur. These failures could partake on any stage along design trajectory of space vehicle. Therefore, research was conducted to identify the probable point in trajectory a space vehicle is most likely to occur. Task was conducted by first finding first and second stage to orbit accidents around the world and creating a histogram, where data involving location and time after launch of accident was recorded. Importance of time of incident is set to determine which areas held highest liability.

After careful evaluation the following Table I was created, which separates data every half a decade displaying all known space vehicle failure within those years and average time incident occur after launch. As shown on Table I, over the last

TABLE I: Historical Points of Incidents

| Year | Number of incidents | Averaged Time of incident |
|---|---|---|
| 1995-1999 | 18 | 53 seconds |
| 2000-2004 | 9 | 143 seconds |
| 2005 -2009 | 13 | 157 seconds |
| 2010 -2014 | 11 | 311 seconds |
| 2015-2019 | 3 | 237 seconds |

twenty years there has been several improvements concerning launch operations making operations much more efficient. Therefore, it is clearly shown that although time of incident would fluctuate there is still a significant difference in number of accidents as well as time after incident in recent years. A histogram for all failure time are summarized in Figure 3. Most failure happens in the first 200 seconds.

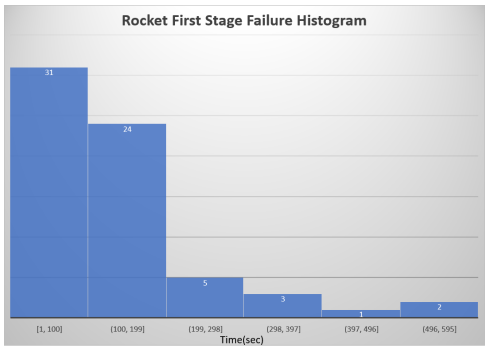


Fig. 3: Rocket first stage failure histogram

### C. Risk Assessment

Understanding the significance of risk level map first requires an understanding why these areas are blocked spaces. Areas closed off to accommodate space launch operations vary according to the launch. This area is assessed using space vehicle specs to determine which range this could possibly have an impact on the NAS. This range could potentially be rather small and closed off for a short period of time, but on instances like SpaceX Falcon Heavy. Due to its large size and vast range of potential debris, over one thousand miles stretching from the cost of Florida over the Atlantic was deemed a no-fly zone with and extended amount of time of nearly 7 hours.

These measures were conducted to assure safety of all air travel through the air space. Although, one major component in creating this risk assessment is the potential debris trajectory there are several factors involved in creating this map, on this paper for the moment we focused on two key factors explained earlier. Figure 4 would contain the basic idea and usage of these risk level map. Figure 4 describes smaller section of a large scale no fly zone, this summarized version still follows the constraints and conditions of large hazard areas. In figure 4, we have three colors red, yellow, and green depicting the risk level of that specific region. Color space red holds the highest risk evaluation while green holds the lowest risk to aircraft.

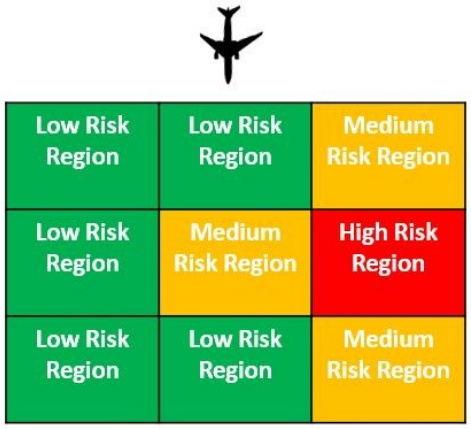


Fig. 4: Concept of risk assessment for hazard area.

To assess the risk to aircraft, we take the three main factors as discussed previously to define a comprehensive risk index:

$$R_{total} = 0.8R_{DM} + 0.2R_{LFP} \tag{9}$$

Using equation above would require to first obtain the two risk levels of each factor. Debris model risk ($R_{DM}$) and launch failure probability risk ($R_{LFP}$) are all levels which need to be assigned to each of the blocks of space within the grid mesh. These are essential to obtain the Total Risk Level per region permitting us to determine which airspace can be partially opened for a partial amount of time, allowing traffic to pass through without having to go around hazard zone.

Different risk tolerance will result in varying size of hazard area. Figure 5 shows the hazard area under different risk tolerance, which are completed using same condition. The aggressive plan, where section is blocked when hit chance is higher than 1/50,000,results in a relative small hazard area, which allows more aircraft pass through. On the other hand, the conservative plan with hit chance 1/1000000 has a much larger hazard area, which forces more aircraft to reroute.

## III. Rerouting Plan Based on Risk Map

Based on the risk assessment, we will propose routing plans to demonstrate the efficiency and performance. This paper takes advantage of A* search algorithm rendering distance and time it takes to go through hazard area created using risk map. For ease of illustration, we simplify our problem to route in a grid rectangle area.

Current method, used by FAA to assure the safety of all aircraft in the proximity, closes a large air space surrounding the set trajectory of the projectile, rendering little to no risk to all air traffic in the surrounding area. Although, this process does appear to be the safest course of action, the extended distant and time of these hazard areas hinders all air traffic greatly costing thousands of dollars per flight proving to be not the most cost efficient.

Shown in figure 6 displayed in red are blocks of space considered no-fly zones created using FAA current method. Previously mentioned this does contain lowest risk to aircraft

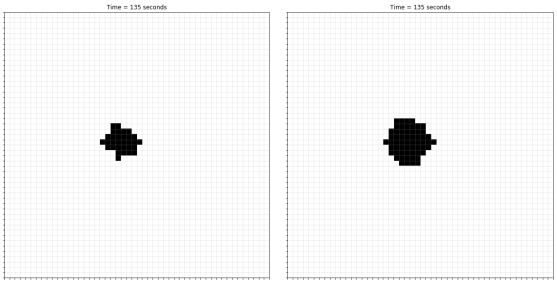


(a) Hit chance 1/50000 (b) Hit chance 1/100000

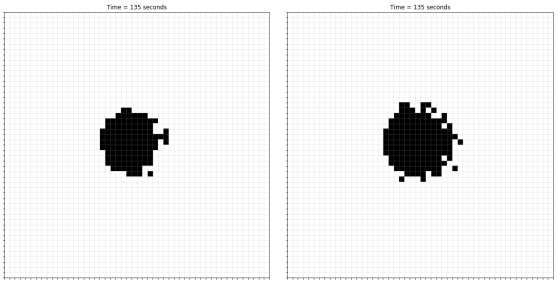


(c) Hit chance 1/500000 (d) Hit chance 1/1000000

Fig. 5: Hazard area under different risk tolerance

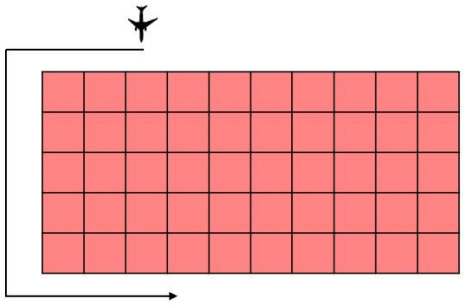

Fig. 6: Concept of reroute around blocked air space.

but hinders overall cost per flight. In this research, distance and time it takes to go through hazard area is also retrieved and compared with our results.

After creating a risk level map, and having all values identified. Closing off blocks of space with a value higher than the set tolerance develops a maze which aircraft would have to navigate through at the lowest expense. Shown in figure 7, the maze is dynamically created based on the current risk level map, where the risk index that is higher than a tolerance level, will be blocked. Then based on the current maze map, search algorithm used in this paper is A* search. [12].

This algorithm does render a much more appropriate approach passing through air space following a shorter and faster way.

## IV. Experiment Results

Recall that we would be using a risk tolerance level to determine which spaces partially open to aircraft. In this research, data retrieved are set to follow original two stage to orbit trajectory with vehicle initial mass equal to max

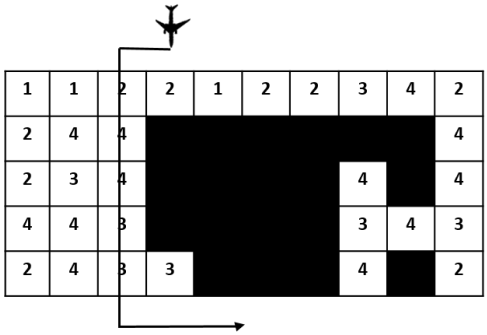


Fig. 7: A* algorithm representation with a tolerance level.

TABLE II: Initial Values at Incident

| Time(s) | Velocity(m/s) | Mass (kg) | Position(m) |
|---|---|---|---|
| 135 | 441.46 | 20508 | [24323, 10607, 0] |
| 140 | 463.71 | 20156 | [26315, 11682, 0] |
| 145 | 486.68 | 19805 | [28397, 12828, 0] |
| 150 | 510.42 | 19453 | [30572, 14048, 0] |

weight minus fuel weight lost and initial speed according to position in time in trajectory. Initial values used are provided in table II. These debris simulations were computed for 10000 simulations to obtain more accurate results when building a grid mesh, each containing randomized mass, velocity and count of debris. Altitude and horizontal distance from launch are shown in table II.

These different points on trajectory renders us different initial conditions for rocket incident. These values are the main source to alternative grid mesh maps, creating different blocked space shifting according to planned trajectory. As expected, during first simulation (the earliest time in rocket path), blocked or closed off blocks of space due to high level risks are directly in front of assigned path of aircraft. Over time, these closed off area could shift to the right aligning the rockets trajectory. After several seconds after launch, blocked spaces are not in the aircrafts proximity, allowing aircraft to follow through directly towards destination. Results proved to be significant, with system being time variant debris projected impacted area would not play into effect the same area as original aircraft assigned route. In figures 8 and 9, the corresponding paths are illustrated in gray line.

Blocked spaces location appears to be dependent on wind direction. Figures 8 and 9 display two different cases with and without wind direction along the rocket trajectory. Images show a clear difference in overall debris impacted area. Process was computed to calculate path around blocked spaces for different wind conditions. Optimal path built for each grid mesh with positive wind direction tends to go around all blocked spaces, circling around with least time consuming cost under required minimum risk level. Similarly, projected hazard areas with no wind are composed of a less spread out hazard zones with a high density of impacted area concentrated directly below point of incident.

Method proposed on this research could significantly reduces travel distance and time than the current method used.

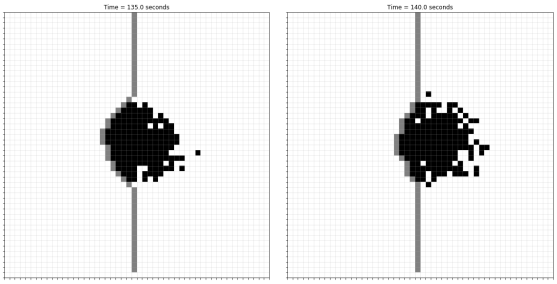


(a) t=135s (b) t=140s

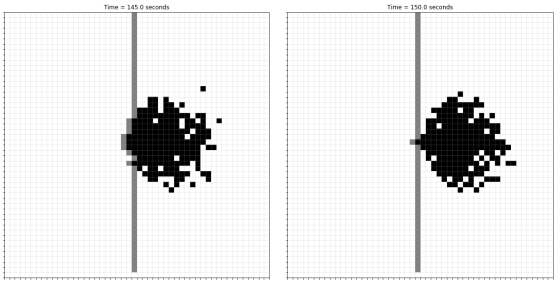


(c) t=145s (d) t=150s

Fig. 8: Hazard area without wind

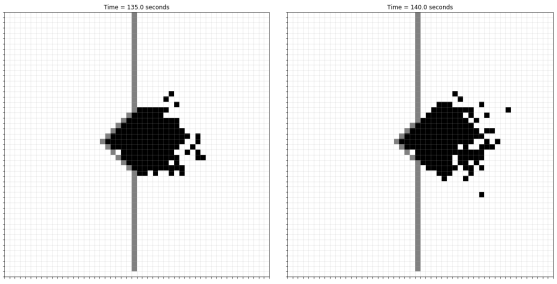


(a) t=135s (b) t=140s

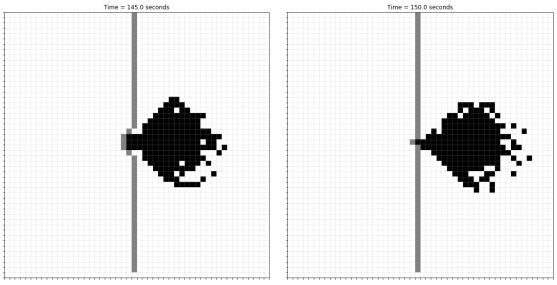


(c) t=145s (d) t=150s

Fig. 9: Hazard area with wind

Utilizing our method aircraft in the proximity have an average of 18.12 percent less distance needed, and 36.6 percent faster than rerouting around hazard area. It minimizes overall cost to air vehicles under required risk level.

## V. Conclusions

In this paper a commercial space launch vehicle and its possible impacts over the national air space is modeled. An overview of decision-making during traffic flow management is provided demonstrating the various methods used in current air traffic rerouting as well as challenges these methods may encounter due to increase of aircraft and space operations. Here a method to construct a risk level map of commercial space launch operations on nearby aircraft is described. Hazard area is divided in multiple sections, each section dynamically evaluated with a risk level. With the use of these proposed sections safety routes are created lowering amount of rerouted aircraft. More importantly, the dynamical updated risk level map could be further transformed to risk probability distribution to enable risk-bounded stochastic planning for air traffic.

## References

[1] D. Murray, "The faas current approach to integrating commercial space operations into the national airspace system," *Federal Aviation Administration*, 2013.

[2] J. Young and M. Kee, *SpaceX Falcon 9/Dragon Operations NAS Impact and Operational Analysis*. Federal Aviation Administration William J. Hughes Technical Center, 2013.

[3] D. Murray and M. Mitchell, "Lessons learned in operational space and air traffic management," in *48th AIAA Aerospace Sciences Meeting Including the New Horizons Forum and Aerospace Exposition*, 2010, p. 1349.

[4] FAA, "Faa aerospace fiscal years 2019-2039," *Federal Aviation Administration*, 2019.

[5] T. J. Colvin and J. J. Alonso, "Compact envelopes and su-farm for integrated air-and-space traffic management," in *53rd AIAA Aerospace Sciences Meeting*, 2015, p. 1822.

[6] AirlinesforAmerica, "U.s. passenger carrier delay costs," *Link: http://airlines.org/dataset/per-minute-cost-of-delays-to-u-s-airlines/*, 2019.

[7] J. Chen, L. Chen, and D. Sun, "Air traffic flow management under uncertainty using chance-constrained optimization," *Transportation Research Part B: Methodological*, vol. 102, pp. 124–141, 2017.

[8] J. Chen and D. Sun, "Stochastic ground-delay-program planning in a metroplex," *Journal of Guidance, Control, and Dynamics*, vol. 41, no. 1, pp. 231–239, 2017.

[9] R. E. Tompa, M. J. Kochenderfer, R. Cole, and J. K. Kuchar, "Optimal aircraft rerouting during commercial space launches," in *2015 IEEE/AIAA 34th Digital Avionics Systems Conference (DASC)*. IEEE, 2015, pp. 9B1–1.

[10] R. E. Tompa and M. J. Kochenderfer, "Optimal aircraft rerouting during space launches using adaptive spatial discretization," in *2018 IEEE/AIAA 37th Digital Avionics Systems Conference (DASC)*. IEEE, 2018, pp. 1–7.

[11] F. M. Capristan and J. J. Alonso, "Range safety assessment tool (rsat): An analysis environment for safety assessment of launch and reentry vehicles," in *52nd Aerospace Sciences Meeting*, 2014, p. 0304.

[12] P. E. Hart, N. J. Nilsson, and B. Raphael, "A formal basis for the heuristic determination of minimum cost paths," *IEEE transactions on Systems Science and Cybernetics*, vol. 4, no. 2, pp. 100–107, 1968.